

single-shower events with  $E_{\text{shower}} > 250$  MeV. The time-of-flight distribution is shown in Fig. 3. We observe no clear in-time signal.

We have performed a Monte Carlo calculation using the Sanford-Wang formula to compare CC rates for the beam dump and bare target. Since  $\pi$  and  $K$  secondary interactions in targets may be important, we calculate rates using an effective  $\pi, K$  absorption length of 30 cm for the beam dump. We assume two cases for the bare target. First, all inelastic pion scatterings remove pions from the beam; and second, there are no pion interactions. In the first case, we are in reasonable agreement with measured yields. In the second case we calculate a beam-dump-to-bare-target event ratio a factor of 2 below what we observe. However, even if one assumes that that discrepancy is due to prompt sources, we can rule out two possibilities. Prompt sources such as charm are expected to yield equal excess of  $\nu_\mu$  ( $\bar{\nu}_\mu$ ) and  $\nu_e$  ( $\bar{\nu}_e$ ) events. We observe no excess  $\nu_e$  ( $\bar{\nu}_e$ ) events over those expected from  $K$  decays and no excess  $\bar{\nu}_\mu$  events over those observed in the bare-target configuration. Neutral penetrating particles interacting in the detector would yield muonless events. We observe no excess NC events for any of the topologies studied.

We use our electron-neutrino rate to set a 90%-confidence-level limit on charm production. Assuming that the invariant cross section for  $D\bar{D}$  production is proportional to  $(1 - |X_F|)^{N_e - b p_A}$ , we calculate an upper limit for the product  $\sigma_{pp \rightarrow D\bar{D}B}$  (cross section times branching ratio to  $\nu_e$ ) of 20  $\mu\text{b}$  for  $N=3$  and  $b=0.5$ ; and 12  $\mu\text{b}$  for  $N=3$  and  $b=2$ . Here we assume the  $A$  dependence for  $D$  production and  $\pi$  production to be the same. The lim-

it is quite independent of the value of  $N$ , since we are sensitive to the low- $|X_F|$  region.

We have used our observed NC rate to set an upper limit on new penetrating particles interacting in our detector. Assuming a production spectrum given by that of the  $\pi$ , we set an upper limit of  $\sigma_{\text{prod}}\sigma_{\text{int}} \leq 5 \times 10^{-68} \text{ cm}^4$  at the 90% confidence level.

If we assume  $\sigma_{\text{int}}^a = \sigma_{\text{prod}}^a = 2.2 \times 10^{-34} \text{ cm}^2$ , we find that  $R = \sigma_{\text{prod}}^a / \sigma_\pi = 1 \times 10^{-8}$ . Using this limit we can calculate the number of in-time single showers expected from the axion decay  $a \rightarrow \gamma\gamma$  in the 50-ft decay space in front of our apparatus as a function of  $c\gamma\tau$ . Assuming an upper limit of three in-time events, we set the limits  $c\gamma\tau > 1 \times 10^9 \text{ ft}$  or  $c\gamma\tau < 12 \text{ ft}$ .

We would like to thank Lou Repeta for construction of the targets and the staff of the AGS for a successful run. S. Marino, E. Druik, and J. Zucker were of great help at various stages of the experiment and the scanning staffs of the University of Illinois and Columbia University did their usual excellent job. This research was supported by the National Science Foundation and the Department of Energy. One of us (P.S.) wishes to thank the Alfred P. Sloan Foundation for support.

<sup>1</sup>P. Alibrand *et al.*, Phys. Lett. **74B**, 134 (1978); T. Hansl *et al.*, Phys. Lett. **74B**, 139 (1978); P. C. Bosetti *et al.*, Phys. Lett. **74B**, 143 (1978).

<sup>2</sup>S. Weinberg, Phys. Rev. Lett. **40**, 223 (1978); F. Wilczek, Phys. Rev. Lett. **40**, 279 (1978).

## Decay Modes of the Isoscalar Giant Quadrupole Resonance in $^{58}\text{Ni}$

M. T. Collins, C. C. Chang, S. L. Tabor, G. J. Wagner,<sup>(a)</sup> and J. R. Wu<sup>(b)</sup>

*Department of Physics and Astronomy, University of Maryland, College Park, Maryland 20742*

(Received 12 March 1979)

Particle decay modes of the giant quadrupole resonance in  $^{58}\text{Ni}$  have been determined in a particle-particle angular correlation experiment. The branching ratios are  $(59 \pm 12)\%$  and  $(12 \pm 4)\%$  [ $(30 \pm 6)\%$  and  $(6 \pm 2)\%$  of the isoscalar  $E2$  energy-weighted sum-rule strength] for proton and  $\alpha$ -particle decay, respectively, and are very similar to those of the underlying continuum and the statistical-model predictions. Our results disagree with a recent electroproduction singles experiment.

Although the isoscalar giant quadrupole resonance (GQR) is the most extensively studied of the "new" resonances discovered after the giant

dipole resonance (GDR),<sup>1</sup> much remains to be understood about it. For example, the GQR is clearly seen in inelastic electron and hadron scat-

tering, but no significant concentration of quadrupole ( $E2$ ) strength has been observed in radiative capture experiments. Whether these two facts are in conflict depends on the ground-state particle decay widths of the GQR.

A recent particle-particle coincidence measurement of the decay of the GQR in  $^{16}\text{O}$  indicated an approximately 100%  $\alpha$ -particle branch.<sup>2</sup> Similar measurements on  $^{40}\text{Ca}$  have yielded branching ratios of  $70_{-20}^{+15}\%$  for protons and  $21_{-15}^{+5}\%$  for  $\alpha$  particles.<sup>3</sup> On the other hand, a singles electroproduction measurement on  $^{58}\text{Ni}$  appears to imply almost 100%  $\alpha$ -particle decay [or  $(56 \pm 4)\%$   $E2$  energy-weighted sum-rule (EWSR) strength] for the GQR.<sup>4</sup> This  $^{58}\text{Ni}$  result is surprising in view of the systematics of decreasing  $\alpha$ -particle branches with increasing  $A$  (and  $Z$ ) and makes a direct coincidence measurement on  $^{58}\text{Ni}$  all the more important. We have made a careful investigation<sup>5</sup> of all the possible particle decay modes of the GQR in  $^{58}\text{Ni}$ .

The reaction  $^{58}\text{Ni}(\alpha, \alpha')^{58}\text{Ni}$  at 140 MeV was used to excite the GQR. Inelastic  $\alpha$  particles were detected at a fixed laboratory angle of  $16^\circ$ . Charged particles from the decay of  $^{58}\text{Ni}$  were detected with 30- $\mu\text{m}$  Si surface-barrier  $\Delta E$  detectors in coincidence with the inelastic  $\alpha$  particles at thirteen angles in and five angles out of the reaction plane. Coincidence neutrons were detected at two angles in a 6-in.  $\times$  5-in. NE213 scintillator using standard  $n$ - $\gamma$  pulse-shape discrimination. Random coincidences have been subtracted from all the coincidence spectra.

The GQR is visible in Fig. 1(a) as a pronounced broad peak at  $E_x \sim 16$  MeV over a significant continuum. To determine the branching ratio of the GQR, this continuum must be subtracted from both the singles and coincidence spectra. Because of the necessarily limited statistics, improved accuracy is obtained by first integrating over angle the various in-plane coincidence spectra (assuming cylindrical symmetry about the recoil direction) and then subtracting an estimated continuum. Figure 1(b) shows the angle-integrated inelastic  $\alpha$ -particle spectrum subject to the condition that a proton of any energy was detected in coincidence. Figure 1(c) was obtained in the same way for  $\alpha$ -particle decay. The inelastic  $\alpha$ -particle spectrum in coincidence with neutron decay at one of the two angles of observation, namely opposite to the recoil axis, is shown in Fig. 1(d).

The fact that a GQR peak is visible in all the coincidence spectra of Fig. 1 shows finite GQR de-

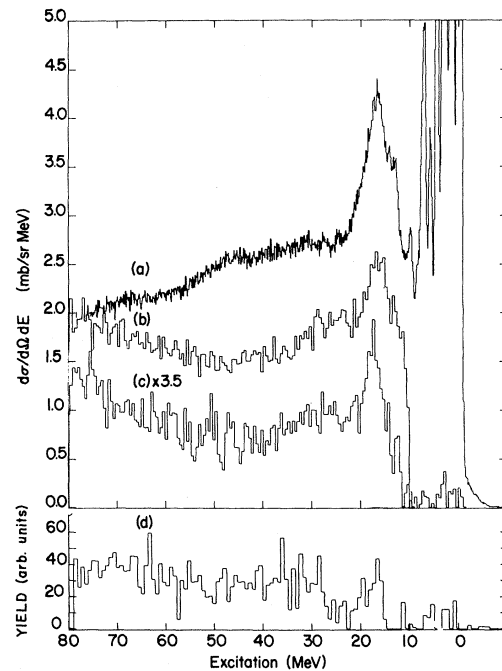


FIG. 1. (a) The inelastic  $\alpha$ -particle spectrum at a laboratory angle of  $16^\circ$  from the reaction  $^{58}\text{Ni}(\alpha, \alpha')^{58}\text{Ni}$  at 140 MeV. The same spectrum is also shown subject to the requirement of (b) a proton, (c) an  $\alpha$  particle, or (d) a neutron coincidence in a second detector. Parts (b) and (c) represent an integration over decay-particle angle as described in the text. The excitation energy refers to the target nucleus,  $^{58}\text{Ni}$ .

decay branches by  $p$ ,  $n$ , and  $\alpha$  emission. The decay branches for the GQR and the underlying continuum deduced from this experiment are listed in Table I. A similar result has also been obtained by Knöpfle *et al.*<sup>6</sup> Uncertainties in the efficiency calibration and the small number of angles measured prevent an accurate determination of the neutron branching ratio. It is, however, consistent with the remaining decay strength.

In a related experiment we have determined the strength of the GQR by comparing the measured singles angular distribution with a DWUCK<sup>7</sup> calculation. Our value of 50% of the isoscalar  $E2$  EWSR strength is in good agreement with previous  $(\alpha, \alpha')$  (Ref. 8) and  $(d, d')$  results.<sup>9</sup> With the use of this number, the GQR decay branching ratios have also been expressed as fractions of the  $E2$  EWSR strength in Table I.

For comparison it is instructive to calculate the branching ratios which would result from the statistical decay of a  $2^+$  state in  $^{58}\text{Ni}$  at  $E_x \sim 16$  MeV, depending on  $Q$  values and barrier penetrabilities. The results, using a modified version

TABLE I. Experimental decay branches in  $^{58}\text{Ni}$  and  $^{40}\text{Ca}$  and statistical-model predictions.

Nucleus	Decay particle	Experiment			
		GQR (%)	Underlying continuum (%)	Hauser-Feshbach $J^\pi = 2^+$ (%)	All $J^\pi$ <sup>c</sup> (%)
$^{58}\text{Ni}$	$n$	...	...	43	38
	$p$	$59 \pm 12$ ( $30 \pm 6$ ) <sup>a</sup>	$53 \pm 10$	51	59
	$\alpha$	$12 \pm 4$ ( $6 \pm 2$ ) <sup>a</sup>	$7 \pm 1$	6	3
$^{40}\text{Ca}$	$n$	...	...	5	6
	$p$	$70^{+15}_{-20}$ <sup>b</sup>	...	74	76
	$\alpha$	$21^{+5}_{-15}$ <sup>b</sup>	...	21	18

<sup>a</sup>Numbers in parentheses represent fraction of isoscalar  $E2$  EWSR strength.

<sup>b</sup>Ref. 3.

<sup>c</sup>Averaged over states of any spin at the GQR excitation energy.

of the Hauser-Feshbach code STATIS with the default values provided for all the relevant parameters,<sup>10</sup> are listed in Table I. It is tempting, on the basis of the good agreement between the statistical-model predictions and experimental decay branches for both  $^{58}\text{Ni}$  and  $^{40}\text{Ca}$  and the similarity between the branching ratios for GQR and underlying continuum, to suggest that the GQR in this mass region decays statistically.<sup>11</sup>

The continuum in Figs. 1(b) and 1(c) under the GQR peak complicates the determination of the GQR decay branches to individual states of the residual nuclei. To see this, let  $E_1$ ,  $E_2$ , and  $E_3$  represent the energies of the scattered particle, the decay particle, and the recoiling nucleus, respectively. From energy conservation, one has  $E_1 + E_2 + E_3 = E_0 - Q_{g.s.} - E_x$ , where  $E_0$  is the incident energy,  $Q_{g.s.}$  is the ground-state  $Q$  value, and  $E_x$  is the excitation energy of the residual nucleus. The recoil energy  $E_3$  is very small and roughly constant. It is observed that the  $E_2$  spectrum for charged particles is a narrow, Maxwellian distribution peaked at the appropriate Coulomb energy, characteristic of an evaporation spectrum. For fixed  $E_x$ , the  $E_1$  spectrum will then be a mirror image of the  $E_2$  spectrum. As  $E_x$  is varied,  $E_1$  will follow it rather closely because the  $E_2$  evaporation spectrum remains roughly invariant.

Figure 2(a) shows the population of excited states in  $^{57}\text{Co}$  following proton decay of  $^{58}\text{Ni}$ . Figure 2(b) shows the projected  $E_1$  spectra for proton decay with windows set on the low-lying states

of  $^{57}\text{Co}$  as indicated on Fig. 2(a). As discussed above, these projections result in a narrow peak which "walks" as the final-state window is moved. Because the narrow peak is no wider than the GQR and walks smoothly through the GQR region, it is difficult to determine what part of the peak results from GQR decay. The projections on the inelastic  $\alpha$ -particle axis for  $\alpha$ -particle decay behave in a similar manner.

The effect of "walking" is also evident in recent GQR decay experiments on  $^{40}\text{Ca}$ .<sup>3,12,13</sup> Windows set on  $\alpha$ -particle decay to the 0-, 2-, and 4-MeV regions in  $^{36}\text{Ar}$  produce  $E_1$  spectra that peak broadly around 14, 16, and 18 MeV of excitation in  $^{40}\text{Ca}$ .

In spite of the difficulty mentioned above, an upper limit of 6% (3% of the  $E2$  EWSR) can be set on the ground-state  $\alpha$ -particle ( $\alpha_0$ ) decay branch of the GQR by not subtracting any underlying continuum. If it is then assumed that the GQR decays in a way similar to the underlying continuum (see Table I), the estimated  $\alpha_0$  branching ratio is 2% (1% of the  $E2$  EWSR). These values are smaller than the value of 4.3% EWSR reported for a capture reaction,  $^{54}\text{Fe}(\alpha, \gamma_0)^{58}\text{Ni}$ .<sup>14</sup> The present total  $\alpha$ -particle decay branch of  $(6 \pm 2)\%$  of the  $E2$  EWSR strength is, however, in serious disagreement with the value of  $(56 \pm 4)\%$  reported for the electroproduction experiment.<sup>4</sup> The question of  $\alpha$ -particle excitation of the GDR has been raised.<sup>4</sup> In order for the  $\alpha$ -particle decay branch to be consistent with that of Ref. 4, one would have to assume that only 10% of the yield observed in the

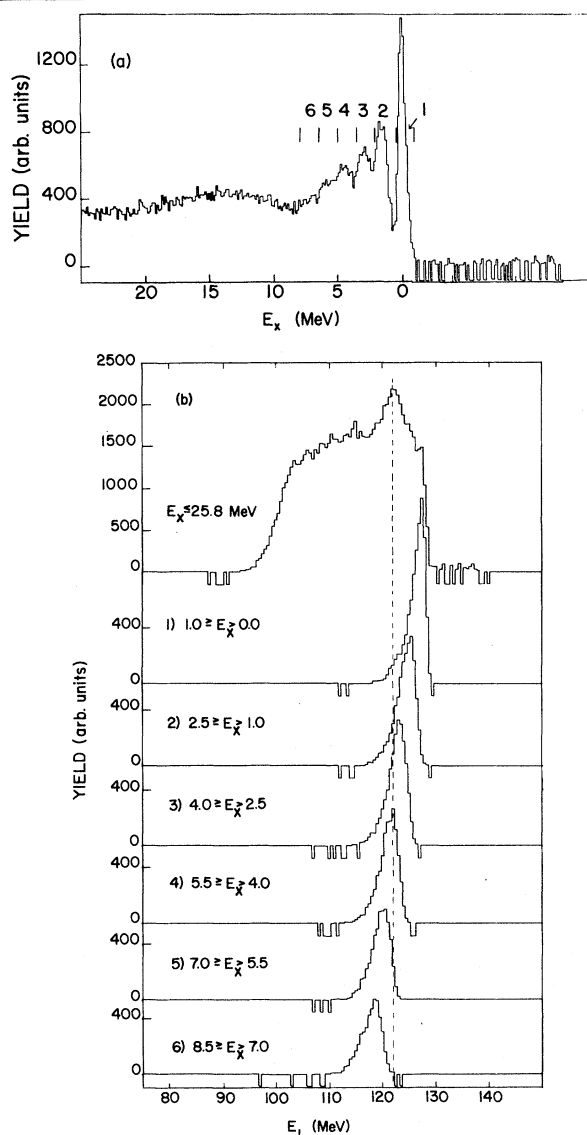


FIG. 2. (a) The population of excited states in  $^{57}\text{Co}$  following proton decay of excited  $^{58}\text{Ni}$ , summed over all angles of observation.  $E_x$  is the excitation energy of  $^{57}\text{Co}$ . (b) The projection of seven regions of (a) on the inelastic  $\alpha$ -particle energy axis. Dips below the zero line indicate the presence (but not magnitude) of negative counts arising from random subtraction.

singles experiment comes from the GQR and the remaining 90%, from the excitation of the GDR. This assumption is inconsistent with the observed  $L=2$  angular distribution<sup>8</sup> and with the  $T=0$  nature of the  $\alpha$  particle. It should be noted that the present experiment is a direct one, while the electroproduction experiment is a somewhat indirect singles measurement. The latter uses a very interesting and novel technique, but the ac-

curacy of the point-nucleus approximation in the calculation of virtual-photon spectrum and the importance of the neglected  $E0$  and  $E3$  components remain to be investigated.

In conclusion, the GQR in  $^{58}\text{Ni}$  has an appreciable proton decay branch and a much weaker  $\alpha$ -particle branch. Neutron decay of the GQR has also been observed. Our total  $\alpha$ -particle decay branch is an order of magnitude smaller than that reported for a recent electroproduction singles experiment. Furthermore, it was observed that the GQR in  $^{58}\text{Ni}$  decays in a way very similar to the underlying continuum and that both are consistent with Hauser-Feshbach predictions. To determine whether this agreement with statistical decay is coincidental or systematic, more experimental data on the decay of the GQR in other nuclei are needed, especially nuclei with quite different particle decay thresholds and penetrabilities. For example, the fact that the evaporation spectrum for neutrons peaks at a much lower energy than for charged particles provides another means of distinguishing between statistical and nonstatistical decay. Detection of neutron decay, whose feasibility has been demonstrated in this work, will also be much more important for the heavy nuclei.

A grant from the University of Maryland Computer Science Center for carrying out part of the calculations is acknowledged. This work was supported in part by the National Science Foundation and is from a dissertation to be submitted to the Graduate School, University of Maryland, by one of us (M.T.C.) in partial fulfillment of the requirements for the Ph.D. degree in Physics.

<sup>(a)</sup>Permanent address: Max-Planck-Institut für Kernphysik, 6900 Heidelberg, Germany.

<sup>(b)</sup>Present address: Oak Ridge National Laboratory, P. O. Box X, Oak Ridge, Tenn. 37830.

<sup>1</sup>F. E. Bertrand, *Annu. Rev. Nucl. Sci.* **26**, 457 (1976).

<sup>2</sup>K. T. Knöpfle, G. J. Wagner, P. Paul, H. Breuer, C. Mayer-Böricke, M. Rogge, and P. Turek, *Phys. Lett.* **74B**, 191 (1978).

<sup>3</sup>D. H. Youngblood, A. D. Bacher, D. R. Brown, J. D. Bronson, J. M. Moss, and C. M. Rozsa, *Phys. Rev. C* **15**, 246 (1977).

<sup>4</sup>E. Wolyneć, *Bull. Am. Phys. Soc.* **23**, 609 (1978); E. Wolyneć, W. R. Dodge, and E. Hayward, *Phys. Rev. Lett.* **42**, 27 (1979).

<sup>5</sup>M. T. Collins, C. C. Chang, S. L. Tabor, J. R. Wu, and M. D. Glascock, *Bull. Am. Phys. Soc.* **23**, 506 (1978).

<sup>6</sup>K. T. Knöpfle, H. Riedesel, K. Schindler, G. J. Wagner, C. Mayer-Böricke, W. Oelert, M. Rogge, and R. Turek, in Proceedings of the International Conference on Nuclear Interactions, Canberra, Australia, 1978, edited by B. A. Robson (Springer, Heidelberg, to be published), and to be published.

<sup>7</sup>P. D. Kunz, code DWUCK4 (unpublished).

<sup>8</sup>D. H. Youngblood, J. M. Moss, C. M. Rozsa, J. D. Bronson, A. D. Bacher, and D. R. Brown, Phys. Rev. C **13**, 994 (1976).

<sup>9</sup>C. C. Chang, F. E. Bertrand, and D. C. Kocher, Phys. Rev. Lett. **34**, 221 (1975).

<sup>10</sup>R. Stokstad, Code STATIS (unpublished).

<sup>11</sup>Because of the difficulties discussed in the next two paragraphs, it is very difficult to determine the angu-

lar correlation of the GQR decay to a particular final state. However, the angular correlation of the GQR and underlying continuum to all final states (limited statistics prevent a reliable background subtraction) is indistinguishable from that of the adjacent continuum.

<sup>12</sup>T. Yamagata, K. Iwamoto, S. Kishimoto, B. Saeki, K. Yuasa, M. Tanaka, T. Fukuda, K. Okada, I. Miura, M. Inoue, and H. Ogata, Phys. Rev. Lett. **40**, 1628 (1978).

<sup>13</sup>A. Moalem, W. Benenson, G. M. Crawley, and T. L. Khoo, Phys. Lett. **61B**, 167 (1976); A. Moalem, Nucl. Phys. **A281**, 461 (1977).

<sup>14</sup>L. Meyer-Schützmeister, R. E. Segel, K. Raghunathan, P. T. Debevec, W. R. Wharton, L. L. Rutledge, and T. R. Ophel, Phys. Rev. C **17**, 56 (1978).

## Electron Scattering from the Ground-State Magnetization Distribution of $^{17}\text{O}$

M. V. Hynes, H. Miska,<sup>(a)</sup> B. Norum, W. Bertozzi, S. Kowalski,  
F. N. Rad, C. P. Sargent, T. Sasanuma, and W. Turchinetz

*Department of Physics, Laboratory for Nuclear Science, Massachusetts Institute of Technology,  
Cambridge, Massachusetts 02139*

and

B. L. Berman

*Lawrence Livermore Laboratory, University of California, Livermore, California 94550*

(Received 30 May 1978)

Elastic electron scattering has been used to determine the transverse form factor of the  $^{17}\text{O}$  ground state in the effective momentum-transfer range  $0.55 \leq q_e \leq 2.8 \text{ fm}^{-1}$ . The data show considerable deviation from single-particle predictions; in particular, a sizable suppression of the  $M3$  and an enhancement of the high- $q$  side of the  $M5$ . Recent shell-model, core-polarization, and meson-exchange calculations are not adequate to explain these effects.

We report here the first measurements of elastic electron scattering from the magnetization density of  $^{17}\text{O}$ . The static magnetic dipole moment ( $-1.894 \text{ nm}$ )<sup>1</sup> being very close to the Schmidt limit ( $-1.913 \text{ nm}$ ) has been viewed as strong evidence for the single-particle nature of this nucleus. In addition, the spectroscopic factor for the  $d_{5/2}$  single-particle component of the ground state as determined by  $(d, p)$  reactions is about 0.9.<sup>1</sup> However, the existence of a sizable quadrupole moment ( $-2.562 e\text{-fm}^2$ )<sup>1</sup> for the ground state of  $^{17}\text{O}$  and the large  $E2$  strengths connecting the ground state to the  $\frac{1}{2}^+$  (0.871 MeV) and  $\frac{3}{2}^+$  (5.083 MeV) states indicate a limit to the usefulness of the extreme single-particle model for this nucleus. These effects can be viewed as due to the nonspherical structure of the  $^{16}\text{O}$  core and its polarization by the odd neutron. Under these circumstances, the  $^{16}\text{O}$  core is expected to in-

fluence the magnetization of  $^{17}\text{O}$ . Electron scattering determines the spatial distribution of the magnetization density and hence provides a severe test of our understanding of the structure of  $^{17}\text{O}$ .

The data were collected at the Massachusetts Institute of Technology-Bates Linear Accelerator using the high-resolution energy-loss spectrometer system.<sup>2</sup> Scattered-electron spectra were measured at three scattering angles,  $90^\circ$ ,  $160^\circ$ ,<sup>3</sup> and  $180^\circ$ .<sup>4</sup> The three  $^{17}\text{O}$  targets used were isotopically enriched BeO foils manufactured at Lawrence Livermore Laboratory.<sup>5</sup> The  $^{17}\text{O}$  isotopic enrichments ranged from about 20 to 85%. Target thicknesses ranged from about 20 to 40 mg/cm<sup>2</sup>. Normalization for most of the  $^{17}\text{O}$  data at each energy was relative to  $^{16}\text{O}$ . For the two highest energy points at  $160^\circ$ , where the  $^{16}\text{O}$  cross section was prohibitively small, normalization